
Monograph:
Edwards, J.B. (1977) The Wider Application of Multi-pass Systems Theory Part 1. Multi-Machine and Multi-Cell Systems. Research Report. ACSE Research Report 61 . Department of Automatic Control and Systems Engineering

---

THE WIDER APPLICATION OF MULTIPASS SYSTEMS THEORY

Part 1. Multimachine and multicell systems

by

J. B. Edwards, B.Sc.(Eng.),M.Sc.,A.M.E.M.E.,C.Eng.,M.I.E.E.

Research Report No. 61

July 1977

THE WIDER APPLICATION OF MULTIPASS SYSTEMS THEORY

Part 1. Multimachine and Multicell Systems

J. B. Edwards,* B.Sc.(Eng.), M.Sc., A.M.E.M.E., C.Eng., M.I.E.E.

Abstract

A general time-(distance-) domain representation of unidirectional multipass processes is presented which describes all previously identified examples[1]. It is then shown that systems of multiple machines in which the signal flow is unidirectional can be simulated by the repeated simulation of a single machine and that such a procedure is described by the same general time-domain formulation. The stability of this multipass simulation sequence, and hence that of the multimachine system, can therefore be investigated analytically using the frequency-response approach previously applied[1] to real-life-multipass processes. It is demonstrated how the approach can be applied also to discretised spatially-distributed processes, provided again that signal flow is unidirectional.

The modelling and analysis techniques presented in this first paper are shown to be unsuitable, however, in the presence of either counterflow signals or feedback controllers which are not of a local nature and uniformly distributed along the process. The identification of these limitations is an important objective and provides the motivation and starting point for a companion paper in which the multipass systems approach is adapted to cope with this much wider class of processes.

* University of Sheffield, Department of Control Engineering, Mappin Street, Sheffield S1 3JD.

List of Symbols and Abbreviations

PRINTER'S NOTE: A bar under a symbol denotes a matrix and the symbol should be printed in heavy type without the bar.

T.F. = Transfer function

T.F.M. = Transfer function matrix.

a = desired spatial rate of change of flame front depth (sinter process).

$\underline{A}$, $\underline{B}$, $\underline{C}$, $\underline{D}$, $\underline{F}$, $\underline{J}$, $\underline{K}_1$, $\underline{K}_2$ = constant coefficient matrices in the time (distance) domain representation.

c_1, c_2 = constant parameters of the steel rolling process.

$\underline{d}$ = process disturbance vector produced by the previous pass.

$\underline{E}(s)$ = matrix of elements = o and exp(-Ls).

f = aerodynamic coefficient.

F_n = tractive effort on n'th vehicle

$\underline{G}(s)$ = T.F.M. of an individual machine, (cell), in a cascade of such machines, (cells).

$\underline{G}_1(s)$ = T.F.M. of a single pass.

$\underline{G}_2(s)$ = T.F.M. of any interpass shaping process.

$H(s)$ = open-loop T.F. of the entire interpass-process loop.

$\underline{I}$ = square, diagonal, unity matrix.

k = gain parameter of sinter process.

k_g, k_h = gains of coal cutter steering controller.

k_p, k_i = proportional and integral gains of local sinter process controllers.

k_1 = gain of controller for steel rolling process, velocity gain of vehicle controller.

k_2 = positional gain of vehicle controller.

ℓ = distance traversed along a particular pass.

ℓ_n = distance travelled by n'th vehicle.

$\Delta\ell$ = cell length.

L = total pass length, process length.

M = mass of vehicle.

n = suffix denoting pass, machine or cell number.

N = total number of passes, machines or cells.

ϕ_n, θ_n = temperature perturbations of the two liquid streams in the n'th cell of the heat exchanger.

$\Delta\theta_n$ = steady-state temperature difference between the two streams.

θ = slope of radius vector describing an excursion around the positive half s-plane.

$R,(\to\infty)$ = length of this radius vector.

s = Laplace variable.

τ = entire solution period for multimachine (multicell) system.

t = time.

T = driver reaction time, time parameter of heat exchanger.

T_i = integral acting time of vehicle and sinter process controllers.

T_m = mechanical time constant of vehicle.

Δt = residence time per cell in sintering process.

$\underline{u}$ = manipulable input vector.

u_n = control applied to nth machine, (cell), wind speed in sinter process.

v = total distance passed.

$v(t)$ = velocity of sinter strand.

w_1, w_2 = liquid flow rate perturbations in heat exchanger.

W = steady-state flow rate.

ω = angular frequency.

ω_o = mechanical natural frequency of steel rolling process.

$\underline{x}$ = state vector.

x_n = headway between n-1 and nth vehicles.

X = measurement delay, distance parameter of heat exchanger.

X_1, X_2 = distance constants of coal cutter steering dynamics.

$\underline{y}$ = output vector disturbing the next pass, via $\underline{E}(s)$ and $\underline{G}_2(s)$.

y_n = depth of flame-front in nth cell of sinter process.

$y_{r,n}$ = desired depth.

$\underline{z}$ = vector of state, output and interpass input variables.

ζ = mechanical damping ratio of steel rolling process.

1. Introduction

The description "Multipass process" has hitherto been restricted to processes operated repetitively over a large number of sweeps (or passes) between which strong interaction occurs. It has previously been shown[1,2] that the small perturbation dynamic behaviour of unidirectional multipass processes can be modelled by means of the transfer-function network of Fig. 1 in which $\underline{G}_1(s)$ describes the dynamics of a single pass of the process in response to the disturbance vector $\underline{d}(s)$ arising from the previous pass. $\underline{E}(s)$ is a matrix of elements = 0 and $\exp(-Ls)$, where L is the pass-length and $\underline{G}_2(s)$ describes any shaping of the output vector $\underline{y}(s)$ between passes. The Laplace transforms in s are taken with respect to the total distance, v, passed where, if n is the pass number and, ℓ, the distance traversed along that particular pass, then

$$v = (n-1)L + \ell \tag{1}$$

The model is valid so long as the transients under investigation occur at distances far from both ends of the pass.

In general $\underline{G}_2(s)$ may, when considered in isolation from $\underline{E}(s)$, take on a non-realisable form as in the case of direction-insensitive interpass smoothing phenomena[2] but otherwise we can put $\underline{G}_2(s) = \underline{I}$ and $\underline{E}(s) = \exp(-Ls)\underline{I}$ by lumping any conventional dynamic or algebraic interpass effects within $\underline{G}_1(s)$ so that the process block diagram reduces to the form shown in Fig. 2.

1.1 A time(distance)-domain formulation.

In general the single-pass process $\underline{G}_1(s)$ will involve not merely the vectors $\underline{d}$ and $\underline{y}$ circulating the interpass loop of Fig. 2 but also a state-vector $\underline{x}$, and a control input vector $\underline{u}$. Control can be based on feedback of current or delayed measurements of state or output or could take a feed-forward format based on previous pass information ($\underline{d}$). A combination of these control techniques is, of course, also possible. A time-(or more precisely, distance-), domain formulation for the process $G_1(s)$ sufficiently general to cover all previously identified unidirectional multipass processes may therefore be expressed thus:

$$\dot{\underline{x}}_n(\ell) = \underline{A}\,\underline{x}_n(\ell) + \underline{B}\,\underline{d}_n(\ell) + \underline{C}\,\underline{u}_n(\ell) \tag{2}$$

$$\underline{y}_n(\ell) = \underline{D}\,\underline{x}_n(\ell) + \underline{F}\,\underline{d}_n(\ell) + \underline{J}\,\underline{u}_n(\ell) \tag{3}$$

$$\underline{u}_n(\ell) = \underline{K}_1 \underline{z}_n(\ell) + \underline{K}_2 \underline{z}_n(\ell - X) \tag{4}$$

$$\underline{z}_n(\ell) = \begin{pmatrix} \underline{x}_n(\ell) \\ \underline{y}_n(\ell) \\ \underline{d}_n(\ell) \end{pmatrix} \tag{5}$$

where X represents the measurement delay distance and $\underline{A}$, $\underline{B}$, $\underline{C}$, $\underline{F}$, $\underline{J}$, $\underline{K}_1$ and $\underline{K}_2$ are constant matrices. (The multipass process description is then completed by the equation

$$\underline{d}_n(\ell) = \underline{y}_{n-1}(\ell) \tag{6}$$

all provided that the interpass process is realisable and therefore embraced by equations 2 to 5). By Laplace transformation and elimination of the unwanted vectors $\underline{x}$, $\underline{u}$ and $\underline{z}$ between equations 2 to 5 the single-pass process transfer-function matrix $G_1(s)$ may be calculated in any specific case. Fig. 3 for instance illustrates the coal-cutter steering process model in its elementary form first examined by the author[1,3] but here enhanced by inclusion of sensor and actuator dynamics. The diagram shows the allocation of state, input and output variables to this second-order process which in general suffers multipass interaction through its height y and tilt a. From Fig. 3 therefore the distance domain description can be expressed:

$$\dot{\underline{x}} = \begin{pmatrix} -1/X_1 & , & 1/X_1 \\ 0 & , & 1/X_2 \end{pmatrix} \underline{x} + \begin{pmatrix} 1/X_1 & , & 1/X_1 \\ 0 & , & 0 \end{pmatrix} \underline{d} + \begin{pmatrix} 0 \\ 1/X_2 \end{pmatrix} u \tag{7}$$

$$\underline{y} = \begin{pmatrix} 0 & , & 1 \\ 0 & , & 1 \end{pmatrix} \underline{x} + \begin{pmatrix} 1 & , & 1 \\ 0 & , & 1 \end{pmatrix} \underline{d} + \begin{pmatrix} 0 \\ 0 \end{pmatrix} u \tag{8}$$

and conventional analog control is based on the law

$$u(\ell) = -k_g d_2(\ell) - k_h x_1(\ell - X) \tag{9}$$

Equations 7, 8 and 9 yield the result

$$\underline{\tilde{y}}(s) = \underline{G}_1(s)\ \underline{\tilde{d}}(s)$$

where $$\underline{G}_1(s) = \frac{1}{\{k_h \exp(-sX)+(1+sX_1)(1+sX_2)\}} \begin{pmatrix} (1+sX_1)(1+sX_2), & (1-k_g + sX_2)(1+sX_1) \\ -k_h \exp(-sX), & (1-k_g + sX_2)(1+sX_1) \end{pmatrix} \tag{10}$$

Another example previously studied in detail[1] is the multipass steel-rolling process* illustrated by the state-variable diagram of Fig. 4 and which is described in the distance domain by the equations:

$$\dot{\underline{x}} = \begin{pmatrix} 0 & \omega_o^2 \\ -1 & -2\zeta\omega_o \end{pmatrix} \underline{x} + \begin{pmatrix} 0 \\ -c_1 \end{pmatrix} d + \begin{pmatrix} 0 \\ 1 \end{pmatrix} u \tag{11}$$

$$y = \begin{pmatrix} -1 & , & 0 \end{pmatrix} \underline{x} + c_2\ d \quad + \quad (o)\ u \tag{12}$$

and

$$u_n(\ell) = k_1\ y_n(\ell - X) \tag{13}$$

from which it is readily shown that

$$\tilde{y}(s) = G_1(s)\ \tilde{d}(s)$$

where, in this case,

$$G_1(s) = \frac{\omega_o^2\ (c_1 + c_2) \quad + 2\zeta\omega_o\ c_2\ s + c_2\ s^2}{s^2 + 2\ \zeta\ \omega_o\ s + \omega_o^2\ \{1 + k_1\ \exp(-sX)\}} \tag{14}$$

, $G_1(s)$ being merely a scalar in this case since there is only one interpass dependence.

It will shortly be demonstrated that other classes of process which are not multipass processes in the physical sense nevertheless share the general mathematical structure described above thus permitting their analysis by multipass theory. Furthermore the T.F.M., $\underline{G}_1(s)$, can often be reduced to scalar form like the last example and like the coal cutter in the special case $k_g = 1.0$ and $X_2 = 0$ (see equation 10). Before proceeding therefore we

* In which the steel strip is rolled repetatively through a single pair of rolls.

first examine the special case of a scalar $\underline{G}_1(s)$.

1.2 The Stability of a Single Multipass Loop.

Opening the interpass loop in Fig. 2 the inverse open-loop transfer-function in this scalar case is clearly

$$H^{-1}(s) = - G_1^{-1}(s) \exp (L\, s) \qquad (15)$$

and with $s = j\omega$, (ω real), the locus of $H^{-1}(s)$ clearly takes a spiral form as illustrated in Fig. 5, the radius vector rotating rapidly anticlockwise about the origin (at one revolution per frequency increment $\Delta\omega = 2\pi/L$) and undergoing gradual modulation since the vector length = $|G_1^{-1}(j\omega)|$. Setting $s = R \exp(j\theta)$, ($R \to \infty$ and $\frac{\pi}{2} > \theta > -\frac{\pi}{2}$) and letting s complete the usual clockwise contour around the right hand half s-plane will generate an equal number of clockwise revolutions about the origin as were produced by ω describing the range $-R < \omega < +R$ and these will clearly have infinite radius. If there are no zeros of $G_1(s)$ in the right hand half s-plane, multipass stability is therefore ensured by siting the critical -1 + jo point inside the annulus shown in Fig. 5 thus requiring that

$$|G_1(j\omega)|^{-1} > 1.0 \quad , \text{ for all real } \omega \qquad (16)$$

This alternative approach of opening the interpass loop rather than the author's usual technique of opening the control loop has been briefly reported before and equation 16 presented without proof. In yielding result (16) this approach has the advantage of generality within the field of scalar multipass systems.

Clearly in the above-mentioned steel rolling example it follows that, if dynamics are neglected, then for stability

$$|(c_1 + c_2) \,/\, \{1 + k_1 \exp(-j\omega X)\}| < 1.0$$

so that

$$k_1 < 1 - (c_1 + c_2) \qquad (17)$$

and, for the stability of the coal cutter reduced to a single interpass loop problem by setting $k_g = 1.0$ and $X_2 = 0$,
it follows that:

$$(1+\omega^2 X_1^2) / \{1+\omega^2 X_1^2 + 2\, k_h(\cos\omega X + \omega X_1 \sin \omega X) + k_h^2\} < 1.0 \qquad (18)$$

which is impossible to achieve with any finite choice of gain k_h. Both results have been previously derived[1] by the alternative method.

2. Multimachine Systems

2.1 The Analogy with Multipass Systems

The time domain formulation expressed by equations 2 to 6, (with time t substituted for distance ℓ), could equally well describe systems of the sort shown in block diagram form by Fig. 6 which shows a chain of identical machines,

each of transfer-function matrix $\underline{G}(s)$, each interacting in an identical manner with one of its two neighbours. The T.F.M. $\underline{G}(s)$ could include the effects of any local control acting on each machine. In such a system however, suffix n denotes machine number and not pass number as previously and the individual subsystems $\underline{G}(s)$ operate in time-parallel in the physical world whereas $\underline{G}_1(s)$ in the multipass system is a single process operated sequentially over long intervals. In simulation, however, there is no reason why an individual $\underline{G}(s)$, representing, say, machine n, should not be run as an individual process over any desired interval τ provided its excitation vector $\underline{y}_{n-1}(t)$, $\{= \underline{d}_n(t)\}$, had been previously stored away for the period τ. Furthermore, if output $\underline{y}_n(t)$ were now stored away in place of $\underline{y}_{n-1}(t)$ for the same period, then the cycle could be repeated. Operated in this way, $\underline{G}(s)$ generates the entire output of each machine individually and sequentially at intervals τ. Fig. 7 clearly describes such a sequential simulation and is identical but for the choice of symbols to the multipass system representation of Fig. 2. Indeed the sequential simulation (as opposed to the physical process) is a multipass process and the stability of the system of Fig. 6 is determined by the stability of the system of Fig. 7 so that such multi-machine systems may be analysed as multipass processes.

This concept is not entirely new and was first brought to the author's attention in conversation with Professor J. L. Douce of the University of Warwick. Whilst significantly widening the scope of multipass systems theory it does nevertheless have important limitations which become obvious when we examine multimachine and multicell systems of a more general class than that shown in Fig. 6. For the moment however we consider an important example to which Fig. 6 is appropriate and for which the approach outlined above is successful.

2.2 A Vehicle Convoy

Consider the convoy illustrated diagramatically in Fig. 8 described by the equation:

$$x_n(t) = \ell_{n-1}(t) - \ell_n(t) \tag{19}$$

$$F_n(t) = M\ddot{\ell}_n(t) + f\dot{\ell}_n(t) \tag{20}$$

where ℓ_n and x_n denote respectively the position of vehicle number n and the headway of its leader, n-1 , F_n is the applied tractive effort and M and f are constant coefficients of inertial and aerodynamic* drag respectively.

* Aerodynamic drag is strictly proportional to $(\text{velocity})^2$ but equation 20 is nevertheless appropriate for small perturbations about a nominal speed.

Suppose vehicle n is controlled only in response to its neighbour n-1 such that

$$F_n(t) = k_1\dot{x}_n(t-T) + k_2\{x_n(t-T) - x_r(t-T)\} \tag{21}$$

where k_1 and k_2 are constant positive gains, $x_r(t)$ is the desired headway, here assumed constant, and T is the fixed reaction time of the driver/control system. Fig. 9 is a block diagram showing the allocation of state-and interpass-variables to this second-order system which clearly exhibits only one interpass loop so that, in accordance with the multipass time-domain formulation of Section 1.1, the system may be described thus, (if reference x_r is ignored):

$$\dot{\underline{x}}(t) = \begin{bmatrix} 0 & 1 \\ 0 & -f/M \end{bmatrix} \underline{x}(t) + \begin{bmatrix} 1 \\ 0 \end{bmatrix} d(t) + \begin{bmatrix} 0 \\ 1/M \end{bmatrix} u(t) \tag{22}$$

$$y(t) = [0 \ , \ -1] \ \underline{x}(t) + [0] \ d(t) + [0] \ u(t) \tag{23}$$

and

$$u(t) = -[k_2 \ , \ k_1] \ \underline{x}(t - T) - k_1 \ d(t - T) \tag{24}$$

and from these equations it is readily shown that the $\underline{G}(s)$ of Fig. 7 is given by the scalar expression:

$$\underline{G}(s) = G(s) = \frac{-\exp(-Ts)(k_1 s + k_2)}{Ms^2 + fs + (k_1 s + k_2)\exp(-Ts)} \tag{25}$$

Application of the general single loop criterion, (16) yields the results that, for the stability of the system, then:

$$f\omega\ (1+T_m^2\omega^2) > 2\ k_2\{(T_m - T_i)\omega\cos T\omega + (1+T_m T_i \omega^2)\ \sin T\omega\} \ , \ f \neq 0 \tag{26}$$

for all real ω, where

$$T_m = M/f \text{ and } T_i = k_1/k_2 \tag{27}$$

and

$$M\omega^2 > 2\ k_2\ (\cos T\omega + T_i\ \omega \sin T\omega) \quad , \ f = 0 \tag{28}$$

again for all real ω.

Although an analytical solution of (26) is not possible in general a number of interesting special case results can be derived from (26) and (28) viz:

Suppose vehicle n is controlled only in response to its neighbour n-1 such that

$$F_n(t) = k_1 \dot{x}_n(t-T) + k_2\{x_n(t-T) - x_r(t-T)\} \tag{21}$$

where k_1 and k_2 are constant positive gains, $x_r(t)$ is the desired headway, here assumed constant, and T is the fixed reaction time of the driver/control system. Fig. 9 is a block diagram showing the allocation of state-and interpass-variables to this second-order system which clearly exhibits only one interpass loop so that, in accordance with the multipass time-domain formulation of Section 1.1, the system may be described thus, (if reference x_r is ignored):

$$\dot{\underline{x}}(t) = \begin{bmatrix} 0 & 1 \\ 0 & -f/M \end{bmatrix} \underline{x}(t) + \begin{bmatrix} 1 \\ 0 \end{bmatrix} d(t) + \begin{bmatrix} 0 \\ 1/M \end{bmatrix} u(t) \tag{22}$$

$$y(t) = [0 \ , \ -1] \ \underline{x}(t) + [0] \ d(t) + [0] \ u(t) \tag{23}$$

and

$$u(t) = -[k_2 \ , \ k_1] \ \underline{x}(t-T) - k_1 \ d(t-T) \tag{24}$$

and from these equations it is readily shown that the $\underline{G}(s)$ of Fig. 7 is given by the scalar expression:

$$\underline{G}(s) = G(s) = \frac{-\exp(-Ts)(k_1 s + k_2)}{Ms^2 + fs + (k_1 s + k_2)\exp(-Ts)} \tag{25}$$

Application of the general single loop criterion, (16) yields the results that, for the stability of the system, then:

$$f\omega\,(1+T_m^2\omega^2) > 2\,k_2\{(T_m - T_i)\omega\cos T\omega + (1+T_m T_i \omega^2)\sin T\omega\} \ , \ f \neq 0 \tag{26}$$

for all real ω, where

$$T_m = M/f \text{ and } T_i = k_1/k_2 \tag{27}$$

and

$$M\omega^2 > 2\,k_2\,(\cos T\omega + T_i\,\omega \sin T\omega) \quad , \ f = 0 \tag{28}$$

again for all real ω.

Although an analytical solution of (26) is not possible in general a number of interesting special case results can be derived from (26) and (28) viz:

Suppose vehicle n is controlled only in response to its neighbour n-1 such that

$$F_n(t) = k_1\dot{x}_n(t-T) + k_2\{x_n(t-T) - x_r(t-T)\} \tag{21}$$

where k_1 and k_2 are constant positive gains, $x_r(t)$ is the desired headway, here assumed constant, and T is the fixed reaction time of the driver/control system. Fig. 9 is a block diagram showing the allocation of state-and interpass-variables to this second-order system which clearly exhibits only one interpass loop so that, in accordance with the multipass time-domain formulation of Section 1.1, the system may be described thus, (if reference x_r is ignored):

$$\dot{\underline{x}}(t) = \begin{pmatrix} 0 & 1 \\ 0 & -f/M \end{pmatrix} \underline{x}(t) + \begin{pmatrix} 1 \\ 0 \end{pmatrix} d(t) + \begin{pmatrix} 0 \\ 1/M \end{pmatrix} u(t) \tag{22}$$

$$y(t) = [0 \ , \ -1] \ \underline{x}(t) + [0] \ d(t) \ + \ [0] \ u(t) \tag{23}$$

and

$$u(t) = -[k_2 \ , \ k_1] \ \underline{x}(t - T) - k_1 \ d(t - T) \tag{24}$$

and from these equations it is readily shown that the $\underline{G}(s)$ of Fig. 7 is given by the scalar expression:

$$\underline{G}(s) = G(s) = \frac{-\exp(-Ts)(k_1 s + k_2)}{Ms^2 + fs + (k_1 s + k_2)\exp(-Ts)} \tag{25}$$

Application of the general single loop criterion, (16) yields the results that, for the stability of the system, then:

$$f\omega\,(1+T_m^2\omega^2) > 2\,k_2\{(T_m - T_i)\omega\cos T\omega + (1+T_m T_i \omega^2)\sin T\omega\} \ , \ f \neq 0 \tag{26}$$

for all real ω, where

$$T_m = M/f \text{ and } T_i = k_1/k_2 \tag{27}$$

and

$$M\omega^2 > 2\,k_2\,(\cos T\omega + T_i\,\omega \sin T\omega) \quad , \ f = 0 \tag{28}$$

again for all real ω.

Although an analytical solution of (26) is not possible in general a number of interesting special case results can be derived from (26) and (28) viz:

(a) for convoy stability , $k_1 < 0.5\ f$, $M = k_2 = 0$

(b) " " " , $k_2 T < 0.5\ f$, $T_i = T_m$

(c) " " " , $k_1 T < 0.5\ M$, $f = k_2 = 0$

and (d) convoy stability cannot be achieved if $f = 0$ and $k_2 \neq 0$, irrespective of the values of M, T and k_1.

The same results are obtainable by the alternative approach of opening the control loop at, say, the point X in Fig. 9 and investigating the resulting open-loop transfer function:

$$G'(s) = \frac{(k_1 + k_2/s)\{1 - \exp(-\tau s)\} \exp(-Ts)}{f(1 + Ms/f)} \qquad (29)$$

where τ = the solution interval, >> T, T_m and T_i. Special case (a), for instance, yields

$$G'(s) = k_1 \{1-\exp(-\tau s)\} \exp(-Ts)/f \qquad (30)$$

the Nyquist plot for which, with $s = j\omega$, the familiar clover-leaf shape shown in Fig. 10. For the infinite semi-circular contour around the positive half s-plane, G'(s) clearly tends to zero and since G'(s) has no poles within the s-contour, for stability, upon closure of the control loop, the critical -1 + j 0 point must lie outside the locus and hence

$$1 > 2\ k_1/f \quad \text{or} \quad k_1 < 0.5\ f,$$

as before.

In a previous paper[1] the stability of a multipass metal rolling process has been considered. In that process, the metal strip passes repeatedly through a single stand rolling-mill but, quite obviously, the same stability conclusions are obtained if the strip is processed by a spatial sequence of identical mills, 0, 1 ... n, ... N, running in time-parallel <u>provided that stand n+1 exercises zero influence on the behaviour of stand n</u> by virtue of, say, interstand tension affecting the strip thickness. Likewise, the approach to the vehicle problem above would have required modification had the control law (equation 21) taken account of the behaviour of both the leading and following vehicles. In such situations neither the time-domain representation of Section 1.1 nor the block diagram of Fig. 6 are applicable because of the counterflow of signals between the individual machines.

3. Multicell Systems

The multimachine approach above may be applied to continuous spatially distributed processes, (within limitations to be identified), if these are first represented by a series of discrete identical cells each described by algebraic and ordinary differential equations.

3.1 An Ore Sintering Process

Consider, for instance, the process illustrated diagramatically by Fig. 11 which shows the downward progress of the flame-front through the ore-coke mixture which is first ignited at the top left hand corner. The burning mixture is conveyed from left to right as shown during the course of combustion, and the object being to achieve complete burn-through at the fixed right-hand end of the process. In Fig. 11, the process has been sub-divided into N conceptual cells. It serves our purpose here to consider control by manipulation of the individual and independently adjustable wind speeds u_1, u_2 ... u_N to which the velocity of the flame-front segments in cells 1, 2 ... N are respectively proportional. An elementary model for the discretised process is simply

$$y_n(t) = y_{n-1}(t) + k\,\Delta t u_n(t) \tag{31}$$

where y_n denotes the depth of the flame front in cell n, k is a constant dependent of mixture permeability and Δt is the residence time of material in any cell. In an attempt to force combustion to follow the desired staircase reference pattern $y_{r,n}(t)$, where

$$y_{r,n}(t) = y_{r,n-1}(t) + a \tag{32}$$

a being a fixed increment, (= depth of bed/N), suppose N local P + I controllers are employed such that

$$u_n(t) = \left[k_p \{y_{r,n}(t) - y_n(t)\} + k_i \int_o^t \{y_{r,n}(t) - y_n(t)\}\right] / k\Delta t \tag{33}$$

then clearly the behaviour of cell n could be computed for any period τ having previously computed and stored the solution $y_{n-1}(t)$, $o < t < \tau$, from cell n-1. The process clearly belongs to the category of Fig. 3 and has the format of Section 1.1. A block diagram for such a sequence of simulations is given in Fig. 12, the stability of which may be determined by examination of the inverse open-loop transfer-function:

$$G^{-1}(s) = \{1 - \exp(-\tau s)\}\, s / \{k_i\,(1 + T_i s)\} \tag{34}$$

where integral-acting time, $T_i = k_p/k_i$ (35)

Now $T_i >> \Delta t$ if the discretising of the process model is to remain valid and $\tau >> T_i$ for a meaningful concept of process stability, viz: the non-propogation of divergent waves along the process irrespective of the observation period. It is readily deduced from the inverse Nyquist diagram that no stability problem exists with this process and provided $k_p \neq 1.0$ no significant transient oscillation will occur either.

Owing to the difficulty in obtaining the necessary N measurements of flame-front depth, distributed feedback control of the sort outlined above is not very practicable generally but could form the basis of a feedforward computer control system for manipulation of the N windboxes in response to synthesized values of $y_1, \ldots y_n, \ldots y_N$. A far simpler technique, however, would involve setting

$$u_n(t) = u_{n+1}(t) = u(t) \quad , \quad 1 \leq n < N \tag{36}$$

and manipulating the single distributed control, u(t), in response to the single point measurement, $y_N(t)$. Alternatively u(t) may be set at a constant value and the conveyor speed v(t) manipulated instead, although the process model, (31) would require adaptation for this situation. The majority of distributed processes are controllable only in this manner, i.e., in a continuous spatial process, the spatial modulation $\underline{f}_1(\ell)$, $0 < \ell < L$, of the distributed control function $\underline{u}(\ell,t) = \underline{f}_1(\ell)\ \underline{f}_2(t)$ is not manipulable and only a single output vector $\underline{y}(\ell',t)$ is available for measurement, ℓ' being some particular value of ℓ. Under such circumstances the nature of the control system renders the process unsuitable for representation by Fig. 3 or by the formulation of section 1.1.

Consider as a second example a symmetrical parallel flow* liquid/liquid heat exchanger conceptually discretised in space and hence described by

$$T\,\dot{\phi}_n(t) = -X\{\phi_n(t)-\phi_{n-1}(t)\}/\Delta\ell + \theta_n(t)-\phi_n(t) + (\Delta\theta_n/W)\{0.6w_1(t)-0.4w_2(t)\} \tag{37}$$

$$T\,\dot{\theta}_n(t) = -X\{\theta_n(t)-\theta_{n-1}(t)\}/\Delta\ell + \phi_n(t)-\theta_n(t) + (\Delta\theta_n/W)\{0.4w_1(t)-0.6w_2(t)\} \tag{38}$$

where ϕ_n and θ_n respectively denote the temperature perturbations in the liquid streams 1 and 2, T and X are quasi-constants depending upon the operating conditions, W denotes the quiesent flow rate of both streams, w_1 and w_2 are the small manipulable perturbations in these, $\Delta\ell$ is the cell length (=L/N), and $\Delta\theta_n$ is the steady-state temperature difference between the two streams. If only open-loop stability studies were required, i.e. $w_1 = w_2 = 0$, then clearly the multimachine approach based on Fig. 3 may be adopted since cells may be computed individually for any period τ in the sequence n = 1, 2 ...N. since the boundary conditions are here fixed at n = 0 $\{\phi_o(t) = \theta_o(t) = 0\}$. The approach as it stands would not be applicable to the controlled system

* Parallel is a term used to describe flows occuring side by side in the same direction, as opposed to the flows occuring in opposite directions and termed counter flows.

however since $\Delta\theta_n$ is non-manipulable and ω_1 and ω_2 are functions only of t thus precluding any form of local control around each cell even if multiple measurements were available for the purpose.

A further problem arises when the counterflow heat exchanger is considered, this being described by

$$T\,\dot{\phi}_n(t) = -X\{\phi_n(t) - \phi_{n-1}(t)\}/\Delta\ell + \theta_n(t) - \phi_n(t) + (\Delta\theta/W)\{0.6\,w_1(t) - 0.4w_2(t)\} \tag{39}$$

$$T\,\dot{\theta}_n(t) = X\{\theta_{n+1}(t) - \theta_n(t)\}/\Delta\ell + \phi_n(t) - \theta_n(t) + (\Delta\theta/W)\{0.4\,w_1(t) - 0.6w_2(t)\} \tag{40}$$

with boundary conditions now fixed at opposite ends of the process, viz:

$$\phi_o(t) = \theta_{N+1}(t) = 0 \tag{41}$$

An added difficulty now arises in that the two-point boundary conditions prevent this process from being computed in a single sequence of simulations for cells 1 to N consecutively. Instead computations must proceed in the form of repetative sweeps in alternate directions, along the process, individual cell computations now being effected for only very short intervals of time. This problem introduced by the counterflow of signals between simulation cells, (and encountered earlier at the end of Section 2.2) further invalidates the generality of the simple approach based on Fig. 3. Some enhancement of the multipass system concept is clearly required for general distributed processes to fall within its scope.

4. Conclusions

It has been shown that multimachine systems and spatially discretised distributed processes can be simulated by a sequence of simulations of merely one machine (or one discrete cell of the process) by first storing the previous output function to provide the subsequent excitation signal. Such a simulation/sequence is a multipass process which may be analysed for stability via, say, the inverse Nyquist method using long time delays to represent the interpass coupling. Stability (or instability) of the multipass simulation implies stability, (or instability), of the real life process. The approach has been successfully applied to a vehicle convoy and an ore-sintering process and indeed could be applied to any multimachine or multicell process in which the signal flow between the individual machine or cell dynamics is unidirectional and any control local to that cell.

The approach outlined in this paper has been shown not to cope with the counterflow of signals between cells (machines) nor with control systems of

a non-distributed, non-local nature. One of the main objectives of this paper has indeed been to identify these very difficulties because their solutions widen the scope of multipass sytems analysis enormously to embrace virtually the whole field of controlled distributed processes. Such difficulties can in fact be overcome quite readily and the methods for so doing are presented in a companion paper[4] for which the present paper is intended to pave the way.

5. References

1. Edwards, J.B., 'Stability problems in the control of multipass processes', Proc. I.E.E., Vol. 121, No. 11, Nov. 1974, pp. 1425-1431.
2. Edwards, J.B. and Greenberg, J.M., 'Longitudinal interactions in multipass processes', Proc. I.E.E., Vol. 124, No.4 April, 1977, pp.385-392.
3. Edwards, J.B. and Bogdadi, W.A., 'Progress in the design and development of automatic control systems for the vertical steering of coal cutters', Proc. I.E.E., Vol. 121, No. 6, pp. 533-536.
4. Edwards, J.B., 'The wider application of multipass systems theory - Part 2, Controlled distributed processes'. Proc. I.E.E.

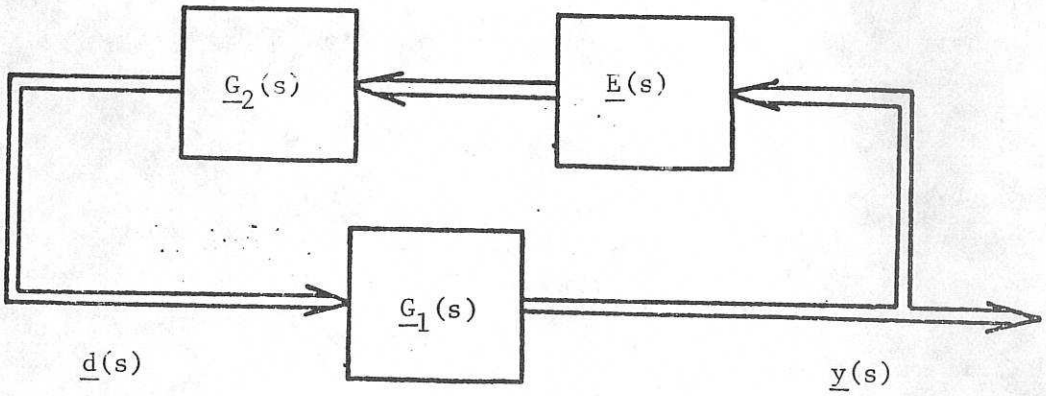

Fig. 1 Transfer function matrix network for a multipass process

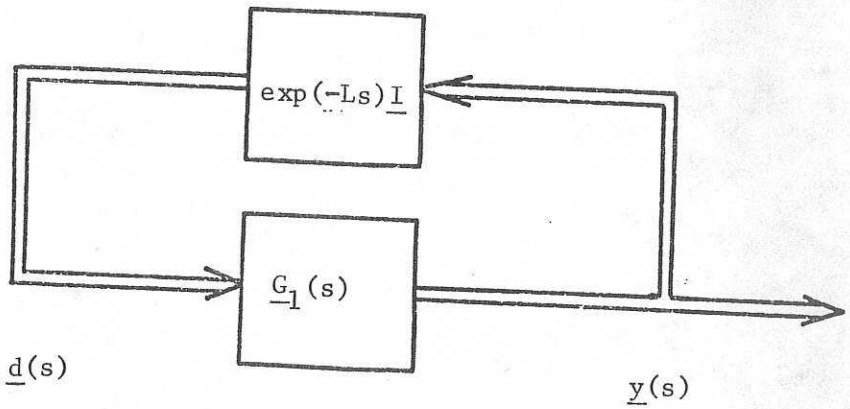

Fig. 2. Reduction of Fig. 1 possible when $\underline{G}_2(s)$ is physically realisable

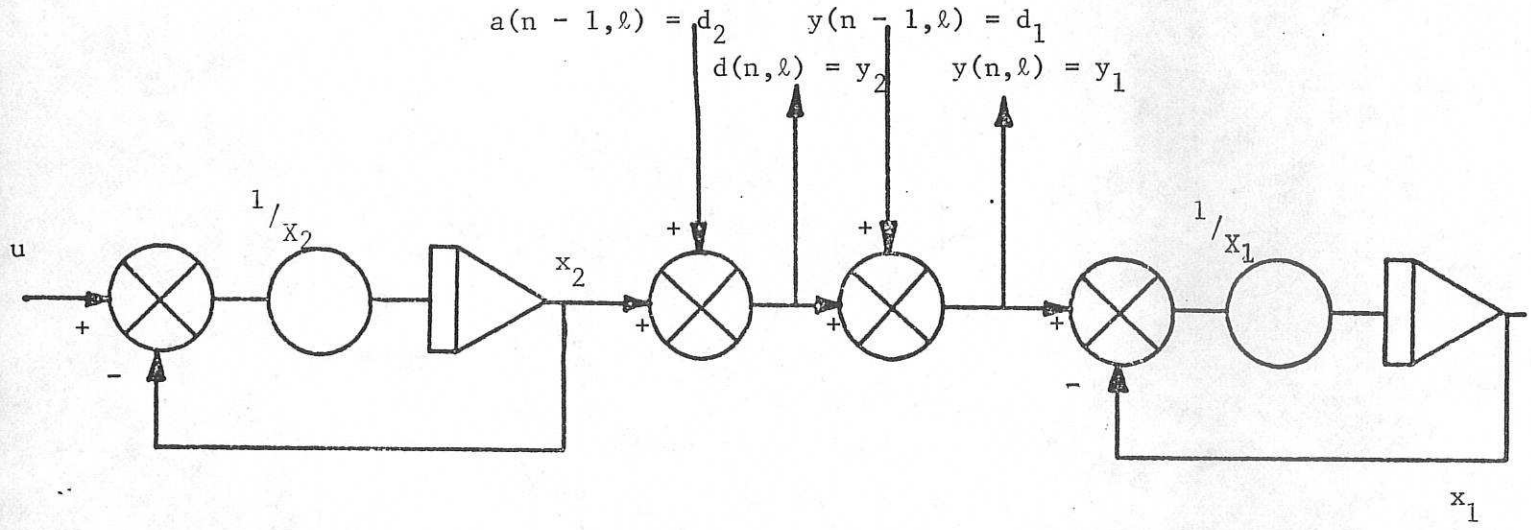

Fig. 3 Showing state, input and output variables for coal-cutter steering process.

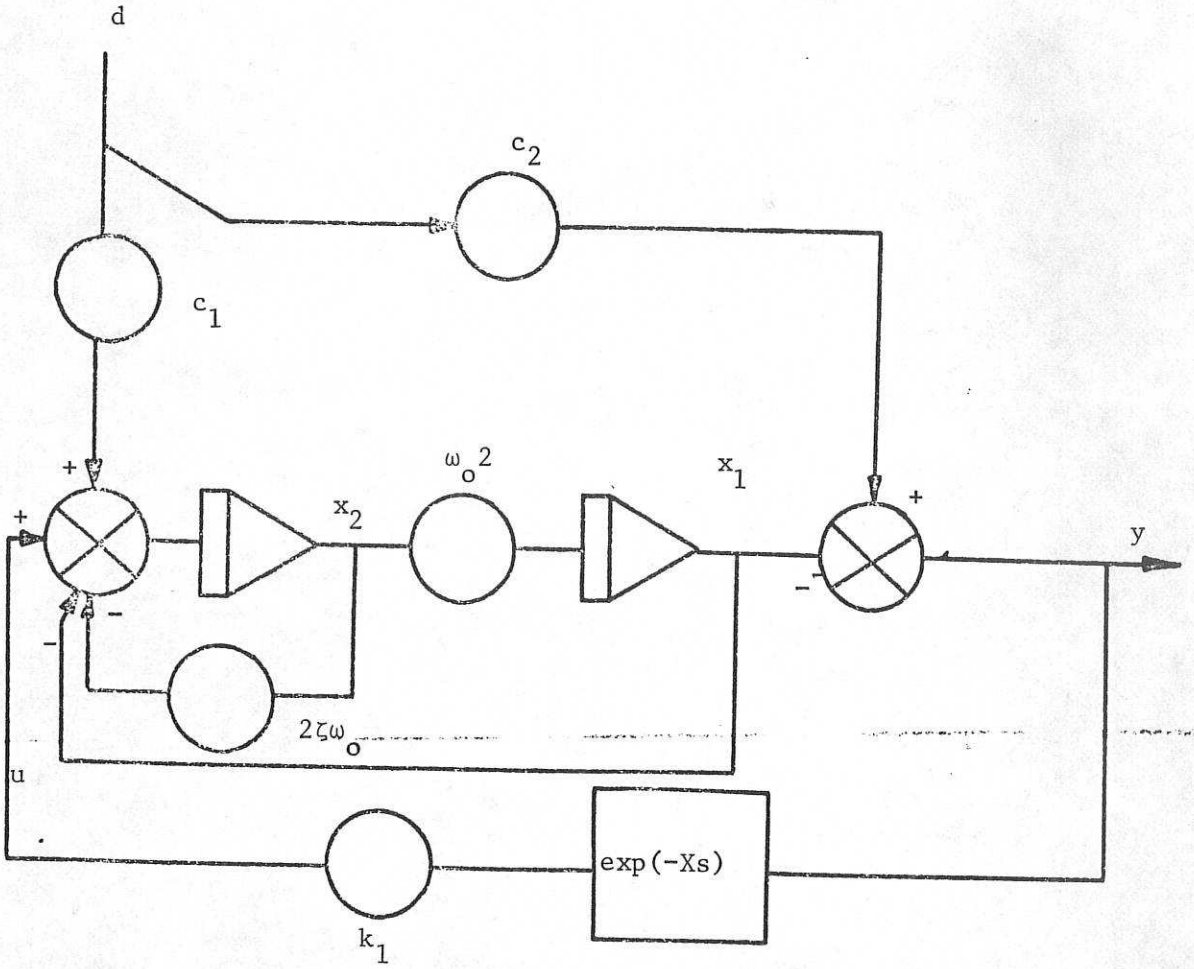

Fig. 4 Showing state, input and output variables for multipass steel rolling process.

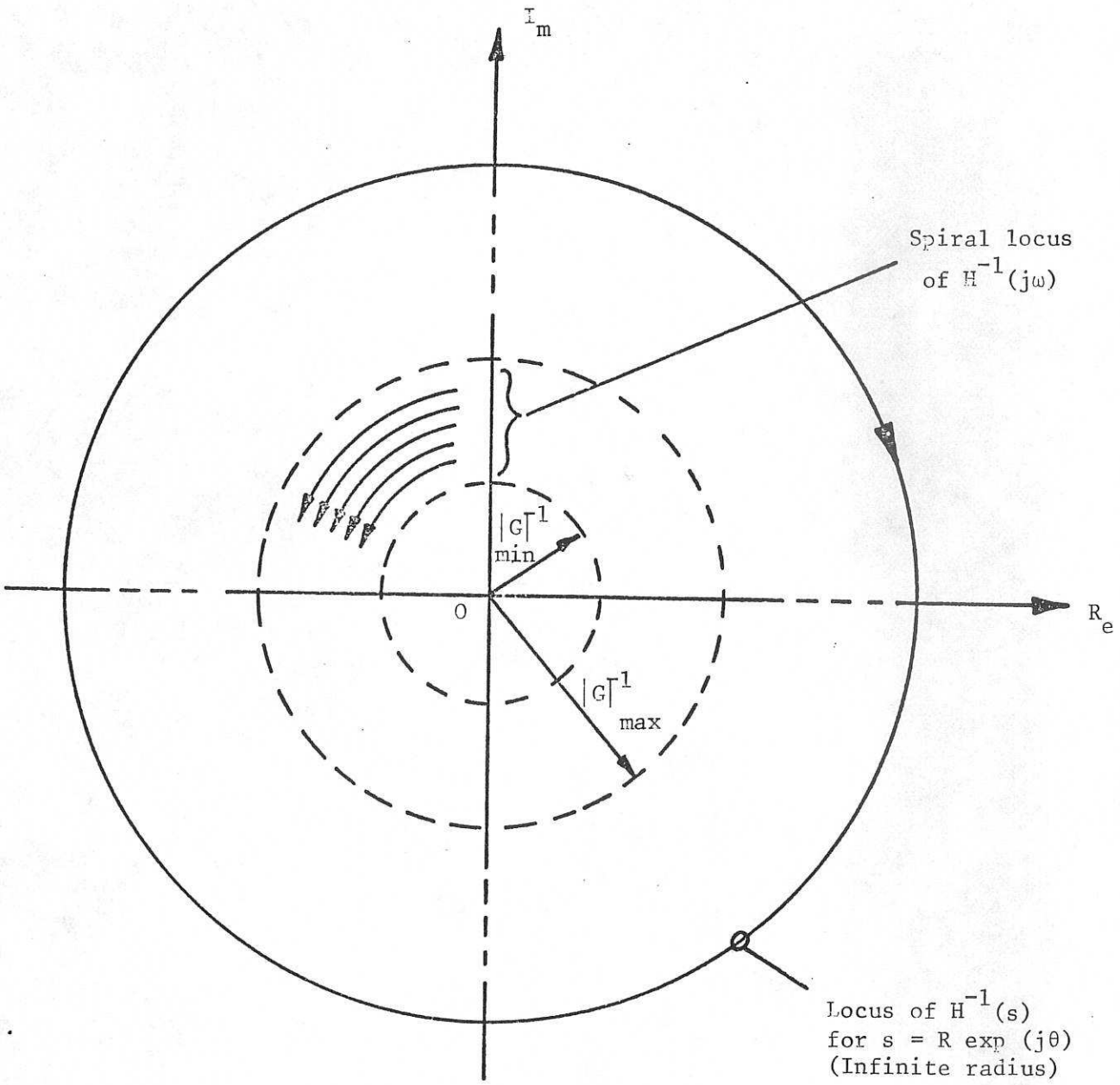

Fig. 5 Inverse Nyquist locus for the complete interpass - process loop.

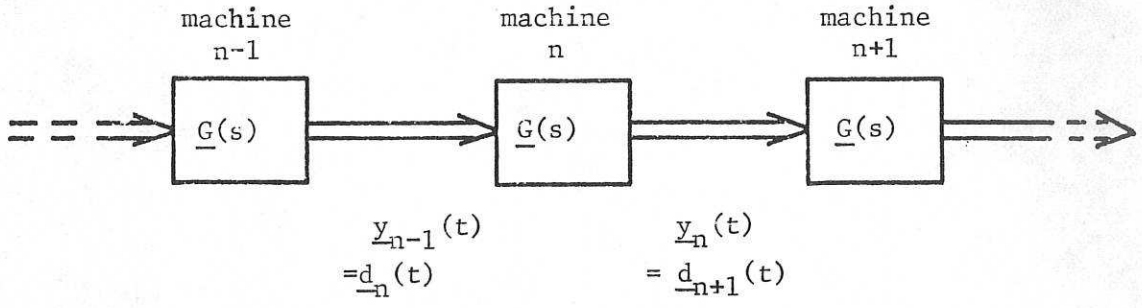

Fig. 6 Illustrating a multimachine chain.

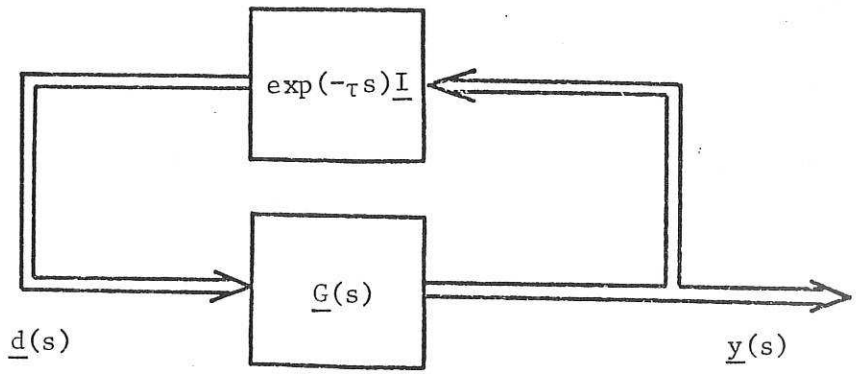

Fig. 7 Representing the sequential solution of the multimachine problem.

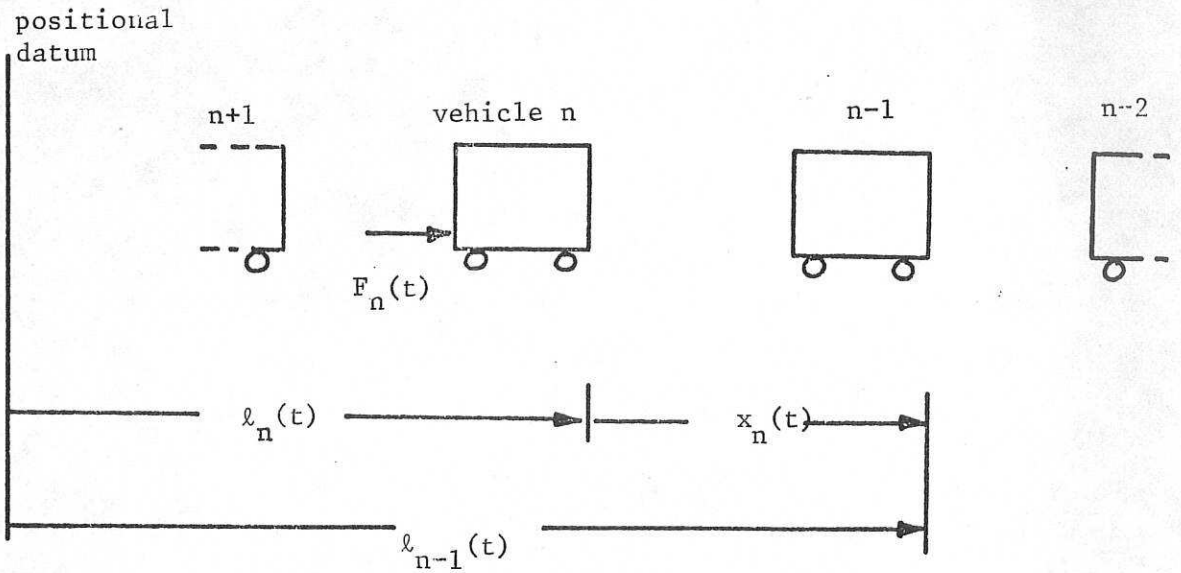

Fig. 8 Convoy of vehicles

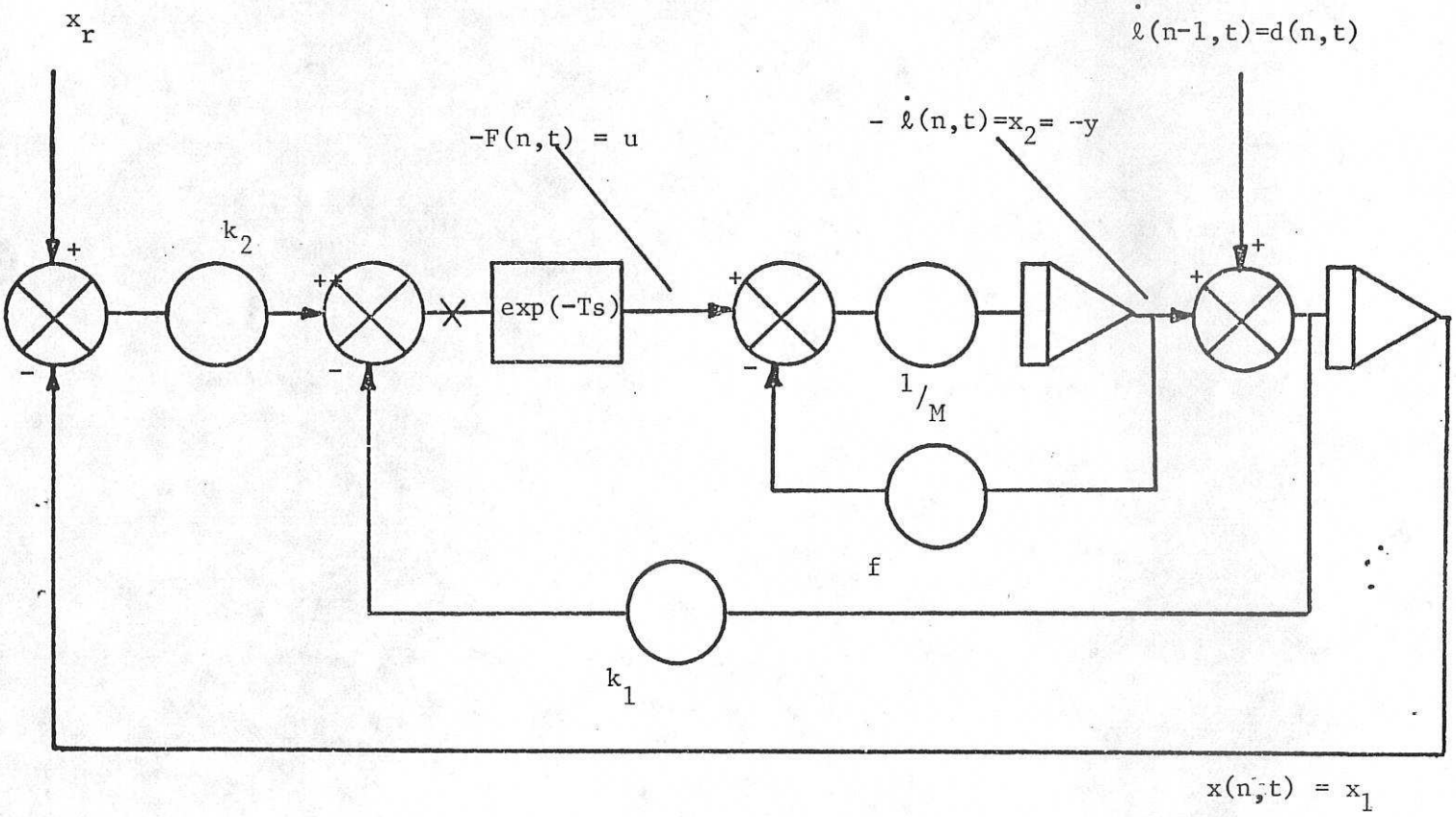

Fig. 9 Showing state, input and output variables for vehicle convoy.

X Indicates point at which control loop is opened for Nyquist analysis.

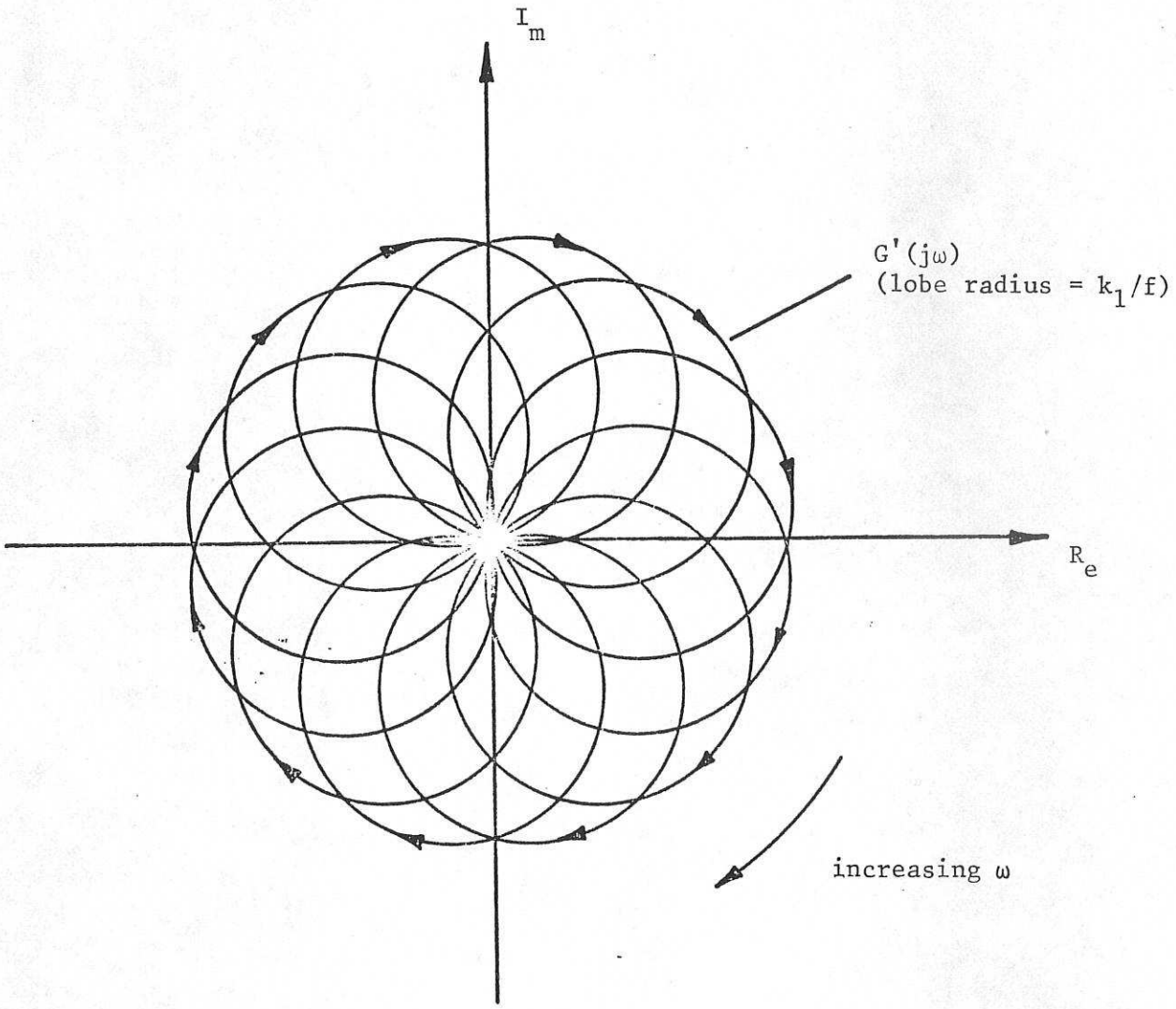

Fig. 10 Nyquist locus for vehicle convoy system

$M = 0$

$k_2 = 0$

$\tau = 12T$

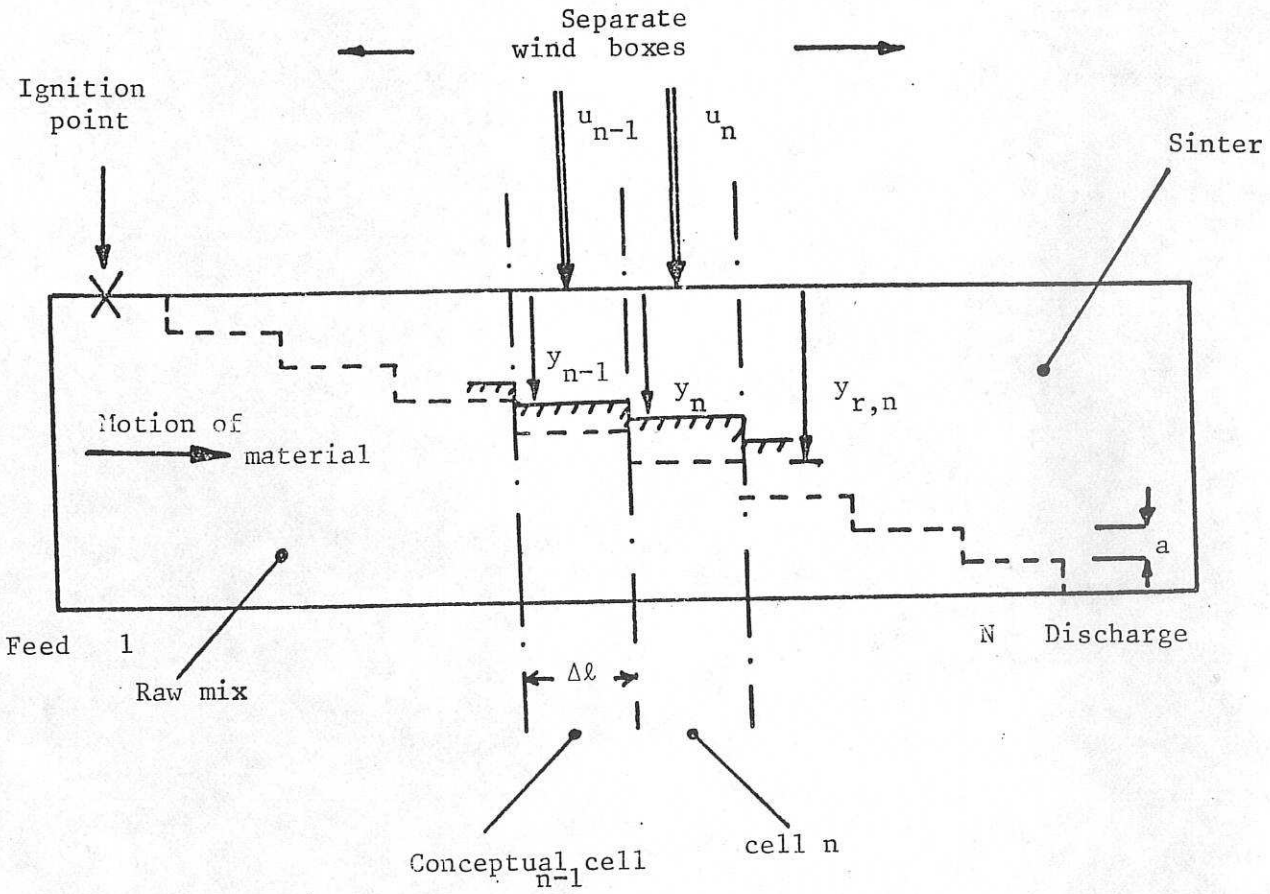

Fig. 11. Illustrating ore sintering process

actual flame front

– – – – desired position of flame front

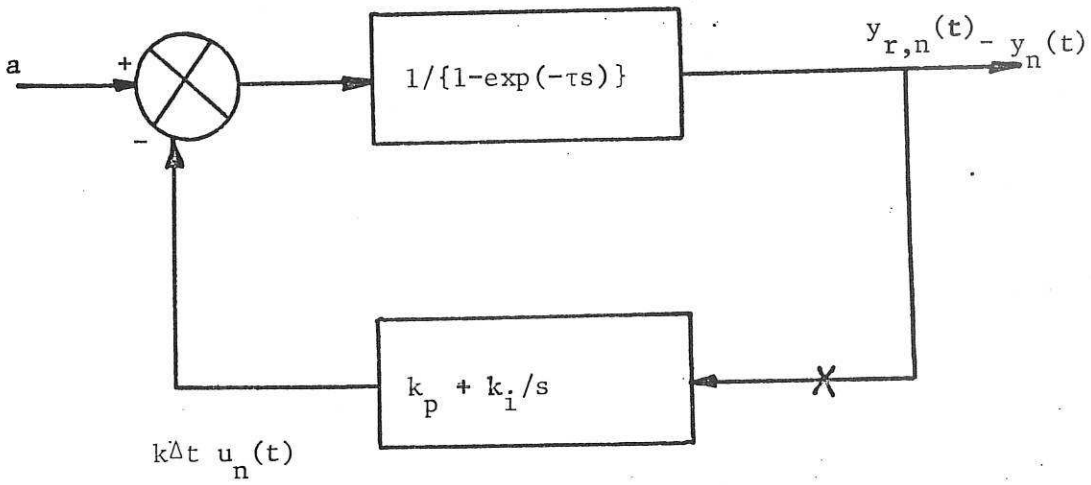

Fig. 12 Block diagram for sequential solution of sinter process

X - loop opened here for inverse Nyquist analysis.